JOURNAL OF MATERIALS SCIENCE 35 (2000) 4735–4741

Electron paramagnetic resonance and Mössbauer spectroscopy of transition metal ion doped mullite

S. P. CHAUDHURI, S. K. PATRA
Special Ceramics Section, Central Glass and Ceramic Research Institute, Calcutta - 700 032, India

Appreciable difference in the properties of undoped and oxide-doped mullite are observed. The oxidation state of cation, its concentration and the position of the mullite lattice occupied by it appear to be the responsible factors. Mullite has, therefore, been doped with four transition metal ions, Mn, Fe, Cr and Ti. With the help of EPR and Mössbauer spectroscopy (supplimented by X-ray diffractometry) the oxidation states of these ions and the mullite lattice sites where they enter has been investigated. It was observed that Mn ion was present in Mn^{2+} and Mn^{3+} states, the former remained as clusters and the latter occupied the octahedral sites in the mullite lattice. Only Fe^{3+} ion was detected and conclusive evidence was obtained for the entry of Fe^{3+} in the octahedral lattice position of mullite from the analysis of Mössbauer spectra with the help of a specially written computer programme. The Cr ion entered the mullite structure only in the Cr^{3+} state. The change in lattice parameters of Cr doped mullite were measured by the XRD technique. The results showed that the expansion of *b*-axis was more than that of the *a*-axis which supported the presence of Cr^{3+} ion in the octahedral site of mullite lattice. The absence of signal in the EPR spectra of Ti doped mullite suggested the presence of only Ti^{4+} ($3d^0$) ion. Very low electrical resistivity of Ti doped mullite and close similarity between mullite and Al_2TiO_5 structures stood as evidence for incorporation of Ti^{4+} ion in the octahedral site of mullite lattice by replacing Al^{3+} ion.

1. Introduction

Mullite ($3Al_2O_3{\cdot}2SiO_2$) has a highly stable [1] but open [2] structure and is characterised by its low density [3] compared to sillimanite, kyanite, etc. It is well-known for its capacity to accommodate several oxides in solid solution [4].

The orthorhombic symmetry of mullite is built up with chains of Al-O octahedra (AlO_6), running parallel to the crystallographic *c*-axis. These are linked by chains of Al-O tetrahedra (AlO_4) and Si-O tetrahedra (SiO_4) (Fig. 1). The connection between the octahedral and tetrahedral chains creates wide channels along the *c*-axis (Fig. 2). The transition metal ions can enter the mullite structure and occupy suitable positions in the octahedral or tetrahedral chains by replacing Al^{3+} ion. Also these ions can occupy the structural channels along the *c*-axis or occupy interstitial locations as clusters. The charge and size [5] of the metal ion and also the crystal system [6, 7] to which the oxide belongs determine [8] the accessible site and the concentration.

The oxides (doping agents) in solid solution in mullite bring about significant changes in properties. The highly enhanced effect of the dopant oxides on the electrical/electronic properties of mullite has been revealed in a very recent work [9]. It becomes possible to decrease the electrical resistivity of mullite by two order of magnitude at room temperature by incorporating transition metal ions, Mn^{2+}, Fe^{3+}, Cr^{3+} and Ti^{4+} into the mullite lattice to the extent of 0.5–2.0 wt.%. It has been further established in another work [10] that the electrical resistivity of mullite can be lowered from 10^{13} ohm-cm at room temperature to less than 10^4 ohm-cm at 1400°C by doping with these ions.

In this paper the dopant ion oxidation state and the mullite lattice site occupied have been identified by EPR and Mössbauer spectroscopy. As supporting evidence, the lattice parameter of pure mullite and Cr doped mullite samples were measured by XRD.

2. Experimental procedure

2.1. Sample preparation

Very pure mullite of composition $3Al_2O_3{\cdot}2SiO_2$ was prepared from aqueous solution of aluminium nitrate nonahydrate,* $Al(NO_3)_3{\cdot}9H_2O$ and tetraethyl orthosilicate solution,† $Si(OC_2H_5)_4$ by mixing them in NH_4OH medium. Aqueous solutions of manganese acetate tetrahydrate,‡ $Mn(CH_3COO)_2{\cdot}4H_2O$, iron

* E. Merck, Germany, 98.5% min.
† BDH Chemicals Ltd., Poole, England, $d^{20^\circ} = 0.933$ g/ml.
‡ Loba Chemie, India, 99.5% min.

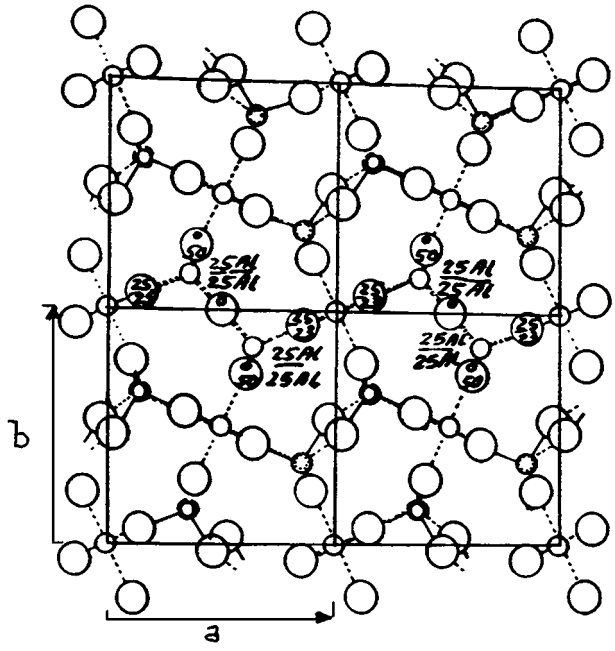

Figure 1 Structure of mullite (after W. H. Taylor [2]). ○ = Al, Si, ○ = Oxygen.

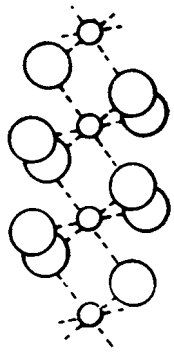

Figure 2 Columns of (AlO_6) octahedra along *c*-axis of mullite, large channels exist in the columns. ○ = Al, ○ = Oxygen.

nitrate nonahydrate,[§] $Fe(NO_3)_3{\cdot}9H_2O$, chromium nitrate nonahydrate,[¶] $Cr(NO_3)_3{\cdot}9H_2O$ and tetraethyl orthotitanate solution,[**] Ti $(OC_2H_5)_4$ were used as sources of Mn, Fe, Cr and Ti, respectively for incorporating in mullite. The hydroxides of Al, Si and dopant ions were coprecipitated from solutions of Al, Si and appropriate dopant ion in NH_4OH medium. After drying the coprecipitate at 120°C, it was calcined at 500°C for 3 h in air. A fluffy, light and reactive powder was obtained that served as mullite precursor. This was finally sintered at 1600°C for 3 h in air to convert it to mullite.

The details of the preparation of doped and undoped mullite samples were reported elsewhere [11].

2.2. EPR spectroscopy

About 25 mg of powdered sample was loaded in the holder of a Varian E-109 X-band EPR spectrometer and the derivative EPR spectrum of the sample was recorded at room temperature and at liquid nitrogen temperature. The observed EPR signals were labelled by their effective $g(g_{\text{eff}})$ values. The g_{eff} of each signal was calculated by the relationship, viz. $g_{\text{eff}} = h\nu/\beta H$, where h, ν, β and H are Plank constant, microwave frequency, Bohr magneton and external field, respectively. The line width (ΔH_{pp}) of each signal was also measured. The external field was varied from 2000–4000 Gauss with the microwave frequency ranging between 9.1 and 9.5 GHz.

2.3. Mössbauer spectroscopy

A standard PC-based set up operating in the constant acceleration mode was used for taking Mössbauer spectra of samples, A 25 mCi ^{57}Co radioactive source in Rh-matrix was employed and measurements were done in transmission geometry at liquid nitrogen temperature.

All the mullite samples were examined by EPR spectroscopy. In addition to this the Fe doped mullite samples were also studied by Mössbauer spectroscopy.

2.4. X-ray diffractometry

The XRD traces of undoped pure mullite (Fig. 3) and Cr doped mullite (Fig. 4) were obtained from 55°–69° (2θ) with Ni-filtered Cu K_α radiation. Six peaks were selected. The positions (2θ) of these peaks for undoped pure mullite and the deviations ($\Delta 2\theta$) of these peak positions for the Cr doped mullite as well as the d-values were calculated.

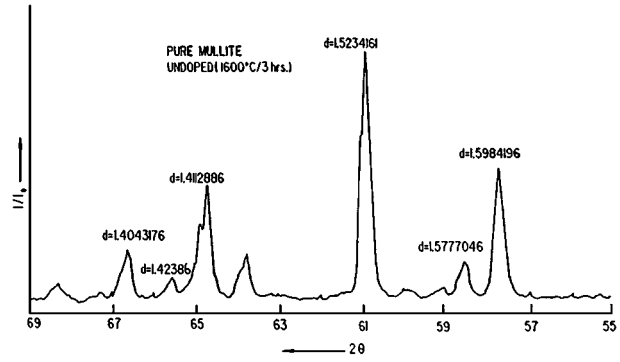

Figure 3 XRD trace of undoped mullite for calculation of unit cell dimension.

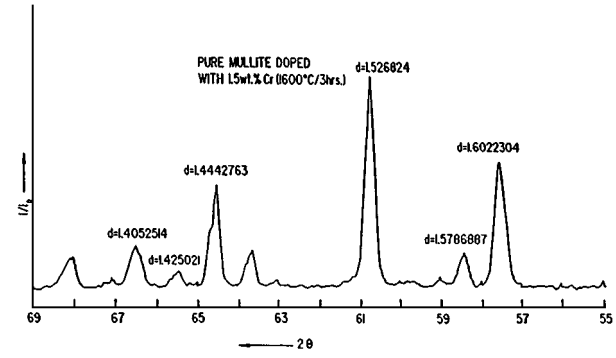

Figure 4 XRD trace of 1.5 wt.% Cr doped mullite for calculation of unit cell dimension.

[§] E. Merck, Germany, 99.0% min.
[¶] Aldrich Chemie, Germany, 99.0% min.
[**] Fluka Chemika, France, $d^{20^\circ} = 1.19$ g/ml.

TABLE I Average lattice parameters of undoped pure mullite with standard deviations, lattice parameters and change in lattice parameters of mullite doped with Cr^{3+} ion

Sample	a_0/(S.D.)	b_0/(S.D.)	c_0/(S.D.)			
Pure Mullite	7.545 ± 0.002 Å/(0.090)	7.687 ± 0.002 Å/(0.110)	2.886 ± 0.002 Å/(0.085)			
	a Å	b Å	c Å	$\Delta a/a_0$ (%)	$\Delta b/b_0$ (%)	$\Delta c/c_0$ (%)
Mullite + 0.5 wt.% Cr	7.538 ± 0.004	7.695 ± 0.004	2.884 ± 0.002	−0.093	+0.156	+0.035
Mullite + 1.0 wt.% Cr	7.538 ± 0.004	7.691 ± 0.004	2.884 ± 0.002	−0.093	+0.104	+0.035
Mullite + 1.5 wt.% Cr	7.538 ± 0.004	7.705 ± 0.004	2.884 ± 0.002	−0.093	+0.286	+0.382
Mullite + 2.0 wt.% Cr	7.538 ± 0.004	7.695 ± 0.004	2.887 ± 0.002	−0.093	+0.156	+0.139

The lattice parameters (a_0, b_0, c_0) of undoped pure mullite, (a, b, c) of Cr-doped mullite and their better estimates were calculated [12–14] by applying the relationships (1) and (2) for the orthorhombic crystals:

$$\frac{1}{d^2} = \frac{h^2}{a^2} + \frac{k^2}{b^2} + \frac{l^2}{c^2} \tag{1}$$

$$\frac{1}{d^2} = \frac{1}{a^2}\left(h^2 + \frac{a^2}{b^2}k^2\right) = \frac{1}{b^2}\left(k^2 + \frac{b^2}{a^2}h^2\right) \quad \text{(assuming } 1 = 0\text{)} \tag{2}$$

The lattice parameters (a_0, b_0, c_0) and their standard deviations, (a, b, c) and $(\Delta a/a_0), (\Delta b/b_0)$ & $(\Delta c/c_0)$, i.e. the changes suffered due to incorporation of Cr in pure mullite are shown in Table I.

3. Results

The EPR spectra of the mullite samples doped with the transition metal ions, Mn, Fe, Cr are shown in Figs 5–7, respectively where a–d stand for 0.5–2.0 wt.% of the same ion, respectively. The calculated g_{eff} values of the signals and their line widths (ΔH_{pp}) for Mn, Fe and Cr doped mullite samples are presented in Tables II–IV, respectively.

TABLE II g_{eff} and ΔH_{pp} values of EPR signals of mullite doped with Mn^{2+} ion

	g_{eff} of EPR signals		ΔH_{pp} of EPR signals (Gauss)	
Sample	I	II	I	II
Mullite + 0.5 wt.% Mn	2.0	—	425	—
Mullite + 1.0 wt.% Mn	2.0	—	440	—
Mullite + 1.5 wt.% Mn	2.0	—	475	—
Mullite + 2.0 wt.% Mn	2.0	1.9	300	325

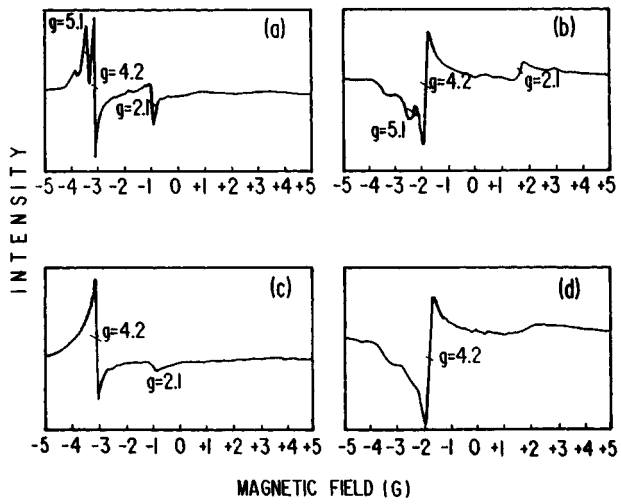

Figure 6 EPR spectra of mullite soped with Fe: (a) 0.5 wt.% Fe, (b) 1.0 wt.% Fe, (c) 1.5 wt.% Fe, (d) 2.0 wt.% Fe.

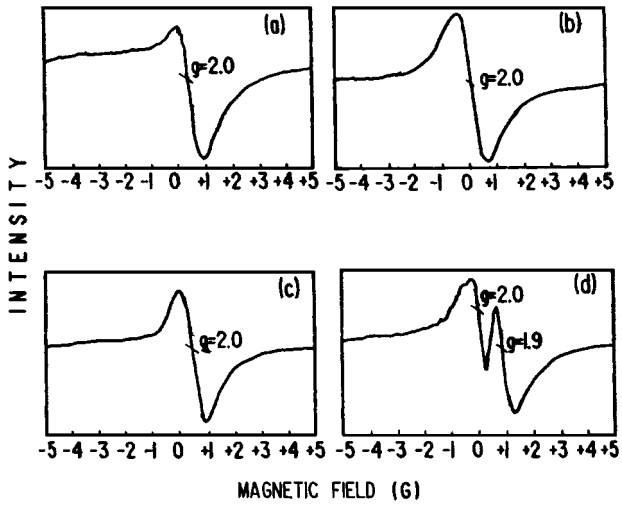

Figure 5 EPR spectra of mullite doped with Mn: (a) 0.5 wt.% Mn, (b) 1.0 wt.% Mn, (c) 1.5 wt.% Mn, (d) 2.0 wt.% Mn.

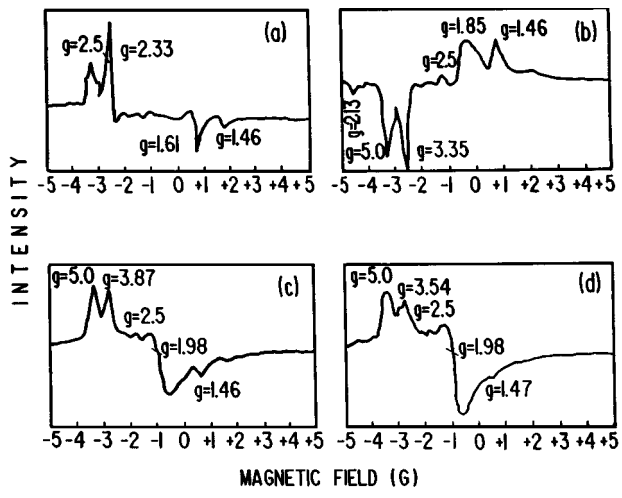

Figure 7 EPR spectra of mullite doped with Cr: (a) 0.5 wt.% Cr, (b) 1.0 wt.% Cr, (c) 1.5 wt.% Cr, (d) 2.0 wt.% Cr.

TABLE III g_{eff} and ΔH_{pp} values of EPR signals of mullite doped with Fe^{3+} ion

Sample	g_{eff} of EPR signals			ΔH_{pp} of EPR signals (Gauss)		
	I	II	III	I	II	III
Mullite + 0.5 wt.% Fe	2.1	4.2	5.1	160	120	120
Mullite + 1.0 wt.% Fe	2.1	4.2	5.1	175	100	100
Mullite + 1.5 wt.% Fe	2.1	4.2	—	200	140	—
Mullite + 2.0 wt.% Fe	—	4.2	—	—	150	—

TABLE IV g_{eff} and ΔH_{pp} values of EPR signals of mullite doped with Cr^{3+} ion

Sample	g_{eff} of EPR signals		ΔH_{pp} of EPR signals (Gauss)	
	I	II	I	II
Mullite + 0.5 wt.% Cr	2.5	—	160	—
Mullite + 1.0 wt.% Cr	2.5	5.0	180	240
Mullite + 1.5 wt.% Cr	2.5	5.0	160	240
Mullite + 2.0 wt.% Cr	2.5	5.0	160	240

In the samples the dopant ions, Mn, Fe and Cr were found to exist in the paramagnetic oxidation states and, therefore, provided EPR signals. No EPR signal was found for the Ti doped samples. This was due to absence of paramagnetic ionic state of Ti.

A EPR signal at $g_{eff} = 2.0$ appeared in the EPR spectrum of each Mn doped mullite sample but there was one more signal at $g_{eff} = 1.9$ in the 2.0 wt.% Mn containing sample. The line widths (ΔH_{pp}) of the signals at $g_{eff} = 2.0$ were above 400 Gauss (425–475) but the ΔH_{pp} of the same signal and also of the signal at $g_{eff} = 1.9$ for the highest Mn containing sample narrowed down to about 300 Gauss (300–325).

A common signal at $g_{eff} = 4.2$ was observed in the EPR spectra of all the Fe doped mullite samples. Besides, two more signals, at $g_{eff} = 2.1$ and the other at $g_{eff} = 5.1$, were detected. The former was present in the samples containing 0.5, 1.0 and 1.5 wt.% Fe and the latter in the first two only. The line wideths (ΔH_{pp}) of the three signals at $g_{eff} = 2.1$, 4.2 and 5.1 varied from 160–200 Gauss, 100–150 Gauss and 100–120 Gauss, respectively. The signal of the smaller g_{eff} was wider than that of the higher g_{eff}.

EPR spectra of Cr doped mullite samples were characterised by two signals at $g_{eff} = 2.5$ and at $g_{eff} = 5.0$. The line widths (ΔH_{pp}) of the two signals in the spectrum of the same sample differed significantly

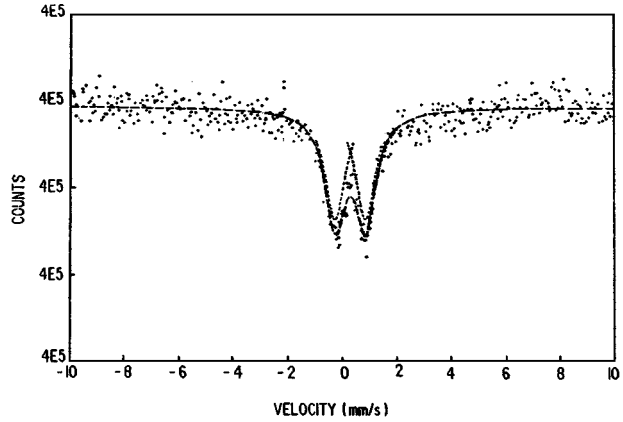

Figure 8 Mössbauer spectrum of mullite doped with Fe.

(160–240 Gauss). But there was no difference in the line widths of the same signals in different samples. The ΔH_{pp} of the signal ($g_{eff} = 2.5$) was about 160 Gauss and that of the signal ($g_{eff} = 5.0$) was 240 Gauss in all the samples, irrespective of different dopant content.

The Mössbauer spectrum of the Fe doped mullite sample (Fig. 8) showed a doublet with large line width. The Lorentzians were fitted and a good χ^2 (1.02) was obtained. It was attempted to fit Mössbauer data to two models, A 1-site model with one doublet having two Lorentzian's lines and a 2-site model with two doublets having four Lorentzian's lines. For the 2-site model there are two types of pairing of lines. For type-I, the 1st line & 3rd line and the 2nd line & 4th line were paired. The 1st line & 3rd line pair corresponds to site-I while the 2nd line & 4th line pair corresponds to site-II. In the type-II pairing, the 1st & 4th lines and 2nd & 3rd lines were paired. Here the pair of 1st & 4th lines corresponds to site-I and the pair of 2nd & 3rd lines corresponds to site-II.

The isomer shift (IS), quadrupole splitting (QS), full width at half maximum (FWHM) and relative intensity values are included in Table V. Assuming

TABLE V Results of Mössbauer spectroscopy of mullite doped with Fe^{3+} ion

Fitting scheme	IS ($\delta \pm 0.02$) (mm/sec.)	QS ($2\epsilon \pm 0.02$) (mm/sec.)	FWHM ($\Gamma \pm 0.02$) (mm/sec.)	Relative intensity (±2%)
"One doublet fit":	0.28	1.14	0.93	38
"Two doublet fit"				
Type-I- 1st and 3rd paired	0.275	1.20	0.92	38
Type-I- 2nd and 4th paired	0.305	1.11	0.92	62
Type-II- 1st and 4th paired	0.306	1.14	0.93	37
Type-II- 2nd and 3rd paired	0.287	1.14	0.93	63

one doublet and two doublet schemes of fitting of Mössbauer data, the range of (IS) and (QS) calculated values were (0.275–0.306) and (1.11–1.20), respectively but (FWHM) values were virtually the same (0.92–0.93).

The lattice parameters of undoped mullite with their standard deviations and the lattice parameters of Cr doped mullite samples are tabulated in Table I. The increase or decrease of lattice parameters due to introduction of Cr in pure mullite are shown in Table I. It was observed that while the *a*-axis of pure mullite contracted, the *b*-axis and *c*-axis expanded at all concentration level (0.5–2.0 wt.%) of dopant Cr. This observation is not consistent with the previous literature [15] in which Nass, *et al*. found that the *a*-axis of mullite doped with Cr_2O_3 expanded more than the *b*-axis per mole of Cr_2O_3 added. This discrepancy was due to the Cr content of mullite. Thus, for Cr doped mullite, $(\Delta b/b_0) > (\Delta a/a_0)$ when the dopant (Cr) content is low as in this study but $(\Delta a/a_0) > (\Delta b/b_0)$ when the dopant (Cr) content is high as in reference [15].

4. Discussion

4.1. Manganese doped mullite

The EPR spectra of these samples (Fig.5) exhibited a broad signal near $g_{\text{eff}} = 2.0$ (Table II) without having any hyperfine structure. It is quite probable that the lack of hyperfine structure indicated the presence of Mn^{2+} ion in the mullite lattice in the form of clusters so that the strong exchange interaction among the component Mn^{2+} ions in each cluster resulted in averaging out the hyperfine structure and a single structureless line was obtained.

Out of the four transition metal ions used in this study Mn^{2+} ion is the biggest (0.80 Å). Due to bulky size, the Mn^{2+} ion could not enter either the octahedral site or the tetrahedral site of mullite. Mn^{2+} ions, thus, exist as clusters.

The other alternative is the occurrence of a Mn-rich phase [16]. The Mn-rich phase would form only when mullite was decomposed and reacted with Mn. This is a remote possibility as because Mn is a good mullite builder [17]. Mn helps formation rather than decomposition of mullite. There appeared no characteristic lines of Mn-Al spinel in the X-ray diffraction profiles of the Mn doped mullite samples. So, Mn did not occur as Mn-rich phase or as Mn-Al spinel in the Mn doped mullite samples.

An additional EPR signal near $g_{\text{eff}} = 1.9$ of line width 325 Gauss appeared in the spectrum of the Mn doped mullite sample of the highest (2.0 wt.%) Mn content (Table II). This was possibly due to the presence of Mn^{3+} ion in octahedral coordination in the mullite structure. With the help of an alternative method, i.e. polarized optical absorption spectroscopy, Schneider [18] and Abs-Wurmbach, *et al*. [19] showed that Mn^{3+} ion entered the octahedral site of Mn doped mullite structure and andalusite structure (very close to mullite), respectively. Oxidation to Mn^{3+} ion can occur during sintering in air. The preference of this site by Mn^{3+} ion is justified because its size (0.58 Å) closely matched the size (0.52 Å) of the octahedral Al^{3+} ion in mullite.

It is important to note that the line width of the spectrum with $g_{\text{eff}} = 2.0$ of the 2.0 wt.% Mn doped mullite sample was significantly less than that of the same spectrum of the samples containing smaller concentrations of Mn (Table II). This has been ascribed to much stronger exchange interaction to effect further narrowing of the spectrum of 2.0 wt.% Mn doped sample.

4.2. Iron doped mullite

More than one signal appeared in the spectra of 0.5, 1.0 and 1.5 wt.% Fe doped mullite samples but only one in the 2.0 wt.% Fe doped mullite sample (Fig. 6). The g_{eff} values of the signals were 2.1, 4.2 and 5.1 (Table III).

Le Marshall, *et al*. [16] investigated the EPR spectra of sillimanite single crystals and mentioned two Fe^{3+} centres with distortion indices, $\lambda = 0.93$ and $\lambda = 0.32$, having $g_{\text{eff}} = 4.2$ and 5.1, respectively. Both these centres were assigned to isolated Fe^{3+} ions occurring at the tetrahedral ($\lambda = 0.93$) and octahedral ($\lambda = 0.32$) lattice positions, respectively, Based on close similarity of mullite and sillimanite crystal structures, the EPR signals of these mullite samples may arise from Fe^{3+} ion. The EPR signals at $g_{\text{eff}} = 4.2$ and at $g_{\text{eff}} = 5.1$ indicated the presence of Fe^{3+} ion in the tetrahedral and octahedral sites of mullite, respectively. The other EPR signal at $g_{\text{eff}} = 2.1$ suggested the existence of Fe^{3+} ion clusters in mullite [20].

Fe^{3+} ion has the electronic configuration of $3d^5$ with spherical charge distribution. This is a stable configuration and shows no preference between octahedral and tetrahedral sites but its behaviour is controlled only by the size of the cations in the lattice. Thus, Fe^{3+} can replace Al^{3+}_{IV} or Al^{3+}_{VI} in mullite. So, the two EPR signals at $g_{\text{eff}} = 4.2$ and 5.1 are justified and the former may be attributed to Fe^{3+} in the tetrahedral site and the latter to Fe^{3+} in the octahedral site of mullite. Saalfeld and Guse [21] also reported similar phenomenon in mullite. In spite of these characteristics of Fe^{3+} ion, its entry in the octahedral site of sintered mullite is favoured but it prefers to occupy the tetrahedral site of fused mullite [22]. Since, here mullite was prepared by sintering the precursor, Fe^{3+} ion occupied mainly the octahedral position.

The observed linewidths (ΔH_{pp}) of the signal at $g_{\text{eff}} = 2.1$ increased with the rise in concentration of Fe^{3+} ion (Table III). This indicated the presence of Fe^{3+} in the distorted octahedral position of mullite, Durán, *et al*. [23] arrived at similar conclusion with the EPR study of Al_2TiO_5 having very close similarity with mullite in structure.

Two broad symmetric lines were found in the Mössbauer spectrum of 2.0 wt.% Fe doped mullite sample (Fig. 8). The large isomer shift was appropriate for Fe^{3+} ion in the octahedral coordination in mullite structure [24]. It may be mentioned that the Mössbauer spectroscope study of Schneider and Rager [20] could not give decisive evidence about the presence of Fe^{3+} ion in the tetrahedral site of mullite.

In the present study, analysis of the strongly overlapping lines in the Mössbauer spectrum was performed by a specific computer programme. In this programme the width and height of a particular Lorentzian can be constrained in specific type. Assuming that there are two sites, site-I and site-II, two doublets or four Lorentzian's lines should be present. So, in type-I analysis, the width and height of 1st & 3rd lines corresponding to site-I and those of 2nd & 4th lines corresponding to site-II were constrained. In type-II analysis those parameters of the 1st & 4th lines corresponding to site-I and the 2nd & 3rd lines corresponding to site-II were constrained. The results of two schemes of fitting (one doublet and two doublets) of Mössbauer data of Fe doped mullite are presented in Table V.

It is found from Table V that for the two doublets scheme of fitting, the isomer shift (IS) and the quadruple splitting (QS) values are nearly equal. This has pointed to the fact that a single site fit is more reasonable in the present study. So, there is only one site in the mullite structure where Fe^{3+} ion has substituted Al^{3+} ion. The tetrahedral substitution by Fe^{3+} required low IS (<0.23 mm/sec.). Therefore, the large isomer shift (IS) (>0.23 mm/sec.) as obtained in the present study (Table V) supported the octahedral substitution by Fe^{3+}. The new scheme of analysis of Mössbauer spectrum, adopted here, confirmed that Fe^{3+} ion occupied the octahedral site of mullite only.

4.3. Chromium doped mullite

There appeared multiple signals in the EPR spectra of Cr doped mullite samples (Fig. 7), particularly at $g_{\text{eff}} = 2.5$ and $g_{\text{eff}} = 5.0$. The signal at $g_{\text{eff}} = 5.0$ resembled that in the EPR spectrum of silicate glass doped with Cr^{3+} ion. This was most possibly due to the presence of isolated Cr^{3+} ion in the strong octahedral crystal field [25]. The signal at $g_{\text{eff}} = 2.5$ indicated that Cr^{3+} ions also entered the interstitial lattice position [25].

With the help of crystal field spectroscopy and EPR measurements, Schneider, *et al*. [26] showed that in mullite precursor at temperatures 1100°C and above the different oxidation states, e.g. Cr^{6+}, Cr^{5+} disappeared but Cr^{3+} remained stable. Thus, in this investigation Cr^{3+} ion got incorporated into mullite lattice because Cr doped mullite was sintered at 1600°C.

Further evidence in favour of substitution of Al^{3+} ion in the (AlO_6) octahedra in mullite lattice by Cr^{3+} ion was acquired by XRD measurement of change of lattice parameters of Cr doped mullite. It has been observed in an earlier investigation [11] that the *c*-axis increased in all the Cr doped mullite samples, the percentage increase ($\Delta c/c_0$) ranged from 0.035% to 0.382%. Similarly, in all the samples the *b*-axis was found to increase much more than the *a*-axis and the percentage increase ($\Delta b/b_0$) varied between 0.104% and 0.286%. But instead of expansion slight contraction took place along *a*-axis to the extent of $(\Delta a/a_0) = -0.093\%$ in all the samples (Table I). It was observed [25, 26] that the substitution of Al^{3+} by Cr^{3+} in the octahedral site of mullite lattice was attended with the expansion of *b*-axis which exceeded that of *a*-axis. The *c*-axis also increased. It may, therefore, be inferred that Cr^{3+} ion went into the octahedral lattice position in mullite.

Confusion was created when *a*-axis was found to increase more than *b*-axis by the substitution of Al^{3+} by Cr^{3+} in mullite in some literature [15]. Concentration of Cr doped in mullite was attributed to this discrepancy. When mullite was doped with low amount of Cr, *b*-axis expanded more than *a*-axis ($\Delta b/b_0 > \Delta a/a_0$) and the *a*-axis expanded more than *b*-axis ($\Delta a/a_0 > \Delta b/b_0$) when high amount of Cr was used as dopant [27, 28].

Beside the present investigation, the EXAFS [29] and time resolved fluorescence spectroscopy [30] studies lend support to the inclusion of Cr^{3+} ion in the octahedral site of mullite structure.

4.4. Titanium doped mullite

No signal was observed in the EPR spectra of Ti doped mullite samples recorded at room temperature as well as liquid N_2 temperature (80° K). So, there was no paramegnetic species of Ti ion in these samples. Ti, therefore, entered the mullite lattice as Ti^{4+} ion ($3d^0$ state).

The presence of Ti^{4+} ion in the octahedral position of Al_2TiO_5 [23] and mullite [25] structures which have very similar orthorhombic structure, was shown by XRD and HREM studies. In previous studies [9, 10] the authors of this communication observed lowest electrical resistivity of Ti doped mullite samples among those investigated and this is consistant with the fact that Ti^{4+} ion substituted Al^{3+} ion in the octahedral site of mullite. This process released one electron from the valence band of Ti^{4+} ion to jump into the conduction band [31], resulting in reduction of the band gap energy. So, the electrical conductivity was remarkably enhanced [10].

5. Conclusions

The investigation of transition metal ion doped mullite by EPR and Mössbauer spectroscopy (and XRD) has led to the following conclusions:

1. Mn occurred as Mn^{2+} and Mn^{3+} ions. Mn^{2+} ions formed clusters and Mn^{3+} ions substituted Al^{3+} ions in the octahedral site of mullite lattice.
2. Fe was found in Fe^{3+} ionic state only. Fe^{3+} ion was located in the octahedral, tetrahedral sites of the mullite lattice and in clusters.
3. Cr was detected as Cr^{3+} ion in the octahedral position of mullite structure. The *b*-axis of mullite expanded more than *a*-axis due to incorporation of Cr into mullite at low concentration level.
4. Ti entered mullite lattice in octahedral site as Ti^{4+} ion.

Acknowledgement

The authors are grateful to Prof. A. K. Pal of Solid State Physics Laboratory of Indian Association for the Cultivation of Science, Calcutta for his help to get the EPR spectra and valuable suggestions. Sincere thanks are due to Dr. D. Das of Inter University Consortium,

Calcutta for his help to get Mössbauer spectra. S. K. Patra thanks CSIR, India for granting him research fellowship to carry out this work.

References

1. R. F. DAVIS and J. A. PASK, in "High Temperature Oxides, Part IV," edited by A. M. Alper (Academic Press, New York, 1990) Ch. 3, p. 37.
2. W. H. TAYLOR, *Z. Krist.* **68** (1928) 503.
3. R. W. G. WYCKOFF, J. W. GREIG and N. L. BOWEN, *Am. J. Sci. 5th Series* **XI**(66) (1926) 459.
4. S. P. CHAUDHURI, *J. Canad. Ceram. Soc.* **58** (1989) 61.
5. N. N. GREENWOOD and A. EARNSHAW, "Chemistry of Elements" (Pergamon Press, Oxford, 1984) Ch. 24.
6. W. D. KINGERY, H. K. BOWEN and D. R. UHLMANN, "Introduction to Ceramics," 2nd ed. (John Wiley, New York, 1976) Ch. 2.
7. H. H. READ, "Rutley's Elements of Mineralogy, Part II," 24th ed. (Thomas Murly & Co., London, 1970).
8. F. A. KRÖGER, "The Chemistry of Imperfect Crystals" (North Holland Publishing Co., Amsterdam, 1964).
9. D. SANYAL, S. K. PATRA, S. P. CHAUDHURI, B. N. GANGULI, D. BANERJEE, U. DE and R. L. BHATTACHARYA, *J. Mater. Sci.* **31** (1996) 3447.
10. S. P. CHAUDHURI, S. K. PATRA and A. K. CHAKRABORTY, *J. Eur. Cream. Soc.* **19** (1999) 2941.
11. S. P. CHAUDHURI and S. K. PATRA, *Brit. Ceram. Trans.* **96** (1997) 105.
12. H. P. KLUG and L. E. ALEXANDER, "X-Ray Diffraction Procedures for Amorphous and Crystalline Materials," 1st ed. (John Wiley and Sons, New York, 1954).
13. B. D. CULLITY, "Elements of X-Ray Diffraction," 2nd ed. (Addison-Wesley, London, 1978).
14. M. K. MURTHY and F. A. HUMMEL, *J. Am. Ceram. Soc.* **43** (1960) 267.
15. R. NASS, E. TKALCEC and H. IVANKOVIC, *ibid.* **78** (1995) 3097.
16. J. LE MARSHALL, D. R. HUTTON, G. J. TROUP and J. R. W. THYER, *Phys. Stat. Sol. (a)* **5** (1971) 769.
17. C. W. PARMELEE and A. R. RODRIGUEZ, *J. Am. Ceram. Soc.* **25** (1942) 1.
18. H. SCHNEIDER, Ph.D. Thesis, University of Münster, Chemistry, FRG, 1986.
19. I. ABS-WURMBACH, K. LANGER, F. SEIFERT and E. TILLMANNS, *Z. KRIST.* **155** (1981) 81.
20. H. SCHNEIDER and H. RAGER, *Ceramics Int.* **12** (1986) 117.
21. H. SAALFELD and W. GUSE, *N. Jb. Miner. Mh.* (1981) 145.
22. W. E. CAMERON, *Phys. Chem. Minerals* **1** (1977) 265.
23. A. DURÁN, H. WOHLFROMN and P. PENA, *J. Eur. Ceram. Soc.* **13** (1994) 73.
24. C. M. CARDILE, W. M. BROWN and K. J. D. MACKENZIE, *J. Mater. Sci. Lett.* **6** (1987) 357.
25. H. SCHNEIDER, in "Ceramic Transactions, Vol. 6: Mullite and Mullite Matrix Composites," edited by S. Somiya, R. F. Davis and J. A. Pask (American Ceramic Society, Westerville, OH, 1990) p. 135.
26. H. SCHNEIDER, K. OKADA and J. A. PASK, "Mullite and Mullite Ceramics" (John Wiley, London, 1994) p. 76.
27. H. RAGER, H. SCHNEIDER and H. GRAETSCH, *Am. Mineral.* **75** (1990) 392.
28. C. GERARDIN, S. SUNDERASAN, J. BENZIGER and A. NOVROTSKY, *Chem. Mater.* **6** (1994) 160.
29. K. R. BAUCHSPIESS, A. KULIKOV and H. SCHNEIDER, in International Workshop-Mullite 94, Irsee, Germany, September 7–9, 1994 Abst. p. 10.
30. B. PIRIOU, H. SCHNEIDER and H. RAGER, *ibid.* Abst. p. 13.
31. S. P. CHAUDHURI, S. BANDYOPADHYAY and N. MITRA, *Interceram* **44** (1995) 300.

Received 9 November 1998
and accepted 7 March 2000